JOURNAL OF MATERIALS SCIENCE 28 (1993) 1885–1900

The effect of surface-limited microcracks on the effective Young's modulus of ceramics

Part I *Analysis*

E. D. CASE, Y. KIM
Department of Metallurgy, Mechanics and Materials Science, Michigan State University, East Lansing, MI 48824-1226, USA

Two types of composite layer model were used to characterize the surface-limited microcrack damage: (i) a dynamic modulus model and (ii) a rule-of-mixtures model. Each model can be applied to either one or two microcracked surface layers for all physically meaningful values of the relative thickness of the layer(s) and all physically meaningful values of the microcrack damage severity states. The microcrack severity can be described in terms of known functions of microcrack size, number density and orientation. A second paper will deal with the details of applying the models to microcracks of a particular geometry, while a third paper deals with experimental tests of the models presented here.

1. Introduction

Microcracks decrease the effective Young's modulus of materials [1–7]. The decrement in Young's modulus is typically described in terms of the average microcrack size, microcrack geometry, and the number density of microcracks for either (i) three-dimensional distributions of microcracks in a body [5–7] or (ii) two-dimensional distributions such as through-cracks in a plate [8–10]. The three-dimensional theories treat either randomly oriented or aligned microcracks [5–7], where the centroid of the crack surfaces are homogeneously distributed in three dimensions. Thus, such theories [5–10] do not treat non-uniform spatial distributions of microcracks, such as the case of a microcrack population limited to a layer near the surface of a brittle specimen.

In ceramics, surface-limited microcrack distributions (that is, distributions of microcracks that occur preferentially in a layer near the specimen's surface) are experimentally observed in (a) machining damage [11–17], (b) indentation [18–23] and (c) impact damage [24–27]. For example, microcracks generated by machining typically appear as two arrays of semi-elliptical cracks with one set parallel to the grinding direction and the other set normal to the grinding direction [11].

In this paper, we consider microcrack–modulus relationships for microcrack damage distributed uniformly within a surface layer or layers. Within the damaged layer, the cracks may be either randomly oriented or preferentially aligned, but beneath the surface damaged layer(s) is a region of the specimen that is microcrack-free. We develop expressions for microcrack-induced modulus changes as measured in uniaxial tension (for which a rule of mixtures (ROM) model can be appropriate, as discussed in Appendix A). We also develop expressions for modulus changes as measured via dynamic modulus measurements (Appendix B). We also discuss the differences between the two techniques in terms of the sensitivity of determining microcracking-induced modulus changes.

2. Layer composite model

In this study, surface-limited microcrack distributions will be modelled in terms of a layered composite, in which a reduced-modulus microcracked outer layer is "bonded" to an undamaged substrate (Fig. 1a and b).

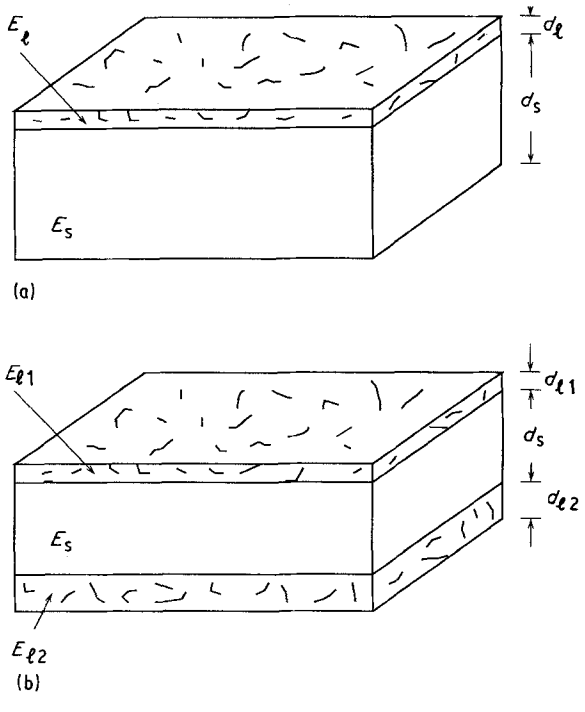

Figure 1 Schematic diagrams of (a) two- and (b) three-layer composite models showing microcracked and microcrack-free layers.

0022–2461

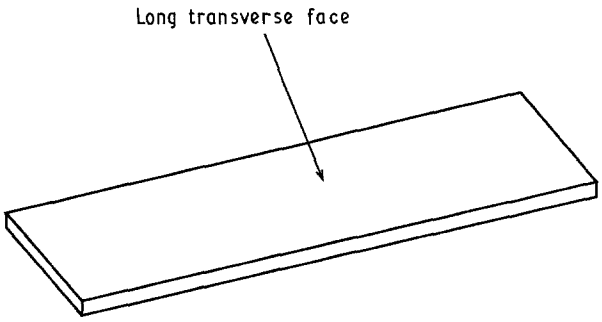

Figure 2 Schematic diagram of long transverse face of sample.

In order to discuss a specific geometry, we shall consider bar-shaped specimens. For example, specimens having microcracks on both long transverse surfaces of a bar (Fig. 2) may be considered as a three-layer composite composed of reduced Young's modulus microcracked layers on the outer transverse surfaces and an undamaged layer between the damaged layers (Fig. 1b).

Within each microcracked layer the change in modulus can be expressed in terms of microcrack number density, orientation and geometry. For a three-dimensional distribution of microcracks in a specimen, where E is the Young's modulus of the microcracked state of the specimen and E_0 is the Young's modulus of the microcrack-free state of the specimen, the relative change in modulus is given by

$$\frac{E_0 - E}{E_0} = \frac{2}{\pi} f G' N_v = f G N_v \quad (1)$$

where f is a function of the spatial orientation of the microcracks [5, 7]. The microcrack geometry factor, G, is given by $2G'/\pi$, where $G' = \langle A^2 \rangle / \langle P \rangle$. $\langle A \rangle$ and $\langle P \rangle$ are the mean microcrack area and the mean microcrack perimeter, respectively. N_v is the crack number density per unit volume of the microcracked body.

Analogous to the case of a three-dimensional microcracked body, for two-dimensional microcrack distributions of through-plate cracks, Equation 1 expresses the modulus change in terms of the size, number density and spatial arrangement of microcracks (See Appendix B of Part II [28]). The form of Equation 1 emphasizes the functional relationships for crack orientation, crack geometry and crack number density which we shall explore in this paper.

Equation 1 is inadequate for the analysis of surface-limited microcrack distributions (Fig. 1a and b), since Equation 1 applies to homogeneous distributions of crack centroids in three-dimensional space [5, 7]. This paper develops a rule-of-mixtures model and a dynamic modulus model for surface-microcracked materials. Within each model, there is a hierarchy of geometries. There is a relative layer geometry factor (the relative thickness of either one or two microcracked surface layers) and a crack geometry/number density factor, expressed in Equation 1 as the product fGN (a function of the orientation, size, shape and number density of the microcracks). This paper develops the relative layer geometry expressions and compares the results for the ROM with dynamic models. Part II [28] treats details of the crack geometry/number density factor, fGN, in terms of application to some "non-standard" crack geometries. Part III [29] gives experimental modulus microcracking results for arrays of indentation-induced surface-limited microcracks in polycrystalline alumina.

2.1. Rule-of-mixtures model

The overall Young's modulus of surface-microcracked specimens can be modelled using the rule of mixtures assuming a two-layer composite having a single microcracked surface layer (Fig. 1a), while a three-layer composite may be used for specimens microcracked on two surfaces (Fig. 1b). The rule-of-mixtures expression for $\bar{E}_{2_{ROM}}$, the overall modulus of a two-layer composite, is

$$\bar{E}_{2_{ROM}} = E_\ell v_\ell + E_s v_s \quad (2)$$

where the subscripts ℓ and s refer to microcrack-damaged layer and undamaged layer, respectively, for the moduli E and volume fraction v (Appendix A).

The rule-of-mixtures expression for $\bar{E}_{3_{ROM}}$, the overall modulus of a three-layer composite, is

$$\bar{E}_{3_{ROM}} = E_{\ell 1} v_{\ell 1} + E_s v_s + E_{\ell 2} v_{\ell 2} \quad (3)$$

where the subscripts $\ell 1$, $\ell 2$ and s refer to the microcrack-damaged layer 1, microcrack-damaged layer 2 and undamaged layer for the moduli E and for the volume fraction v, respectively (Appendix A).

For the three-layer composite model, the elastic modulus for each of the two microcrack-damaged layers can be expressed as [5–7]

$$E_{\ell 1} = E_s(1 - f_1 G_{\ell 1} N_{\ell 1}) = E_s(1 - \Lambda_1) \quad (4a)$$

$$E_{\ell 2} = E_s(1 - f_2 G_{\ell 2} N_{\ell 2}) = E_s(1 - \Lambda_2) \quad (4b)$$

where $\Lambda_i = f_i G_{\ell i} N_{\ell i}$ for $i = 1, 2$. Using Equations 4a and b, $\bar{E}_{3_{ROM}}$ may be expressed as

$$\frac{\bar{E}_{3_{ROM}}}{E_s} = (1 - f_1 G_{\ell 1} N_{\ell 1}) v_{\ell 1} + (1 - v_{\ell 1} - v_{\ell 2}) + (1 - f_2 G_{\ell 2} N_{\ell 2}) v_{\ell 2} \quad (5)$$

where $N_{\ell 1}$, $N_{\ell 2}$ = number density of cracks in microcracked layer 1 and 2, respectively, $N_{\ell 1} v_{\ell 1} = N_{v1} = n_{\ell 1} / V_{specimen}$, $N_{\ell 2} v_{\ell 2} = N_{v2} = n_{\ell 2} / V_{specimen}$, $n_{\ell 1}$ = number of cracks in microcracked layer 1 and $n_{\ell 2}$ = number of cracks in microcracked layer 2. Therefore, the general expression for the fractional change in Young's modulus is

$$\frac{E_s - \bar{E}_{3_{ROM}}}{E_s} = f_1 G_{\ell 1} N_{\ell 1} v_{\ell 1} + f_2 G_{\ell 2} N_{\ell 2} v_{\ell 2} \quad (6)$$

The general form of the ROM model for the three-layer model (two microcracked layers) is a simple sum of the contributions from microcracked layer 1 and from microcracked layer 2. This result, of course, presupposes that there is no interaction between the two crack populations. Lack of crack interaction means, in turn, that the crack number density is sufficiently dilute, but the microcrack-modulus models

described by Equation 1 already assume a dilute population of microcracks [5–7].

If the crack geometry (shape and size) and crack alignment are the same for microcracked layers $\ell 1$ and $\ell 2$, then $f_1 = f_2 = f$ (where equivalent f_i implies equivalent crack alignment) and $G_{\ell 1} = G_{\ell 2} = G_\ell$ (equivalent crack geometry) and thus

$$\frac{E_s - \bar{E}_{3_{ROM}}}{E_s} = fG_\ell(N_{\ell 1}v_{\ell 1} + N_{\ell 2}v_{\ell 2}) = fG_\ell(N_{v1} + N_{v2}) = fG_\ell N_v \quad (7)$$

where $N_{v1} + N_{v2} = (n_{\ell 1} + n_{\ell 2})/V_{specimen} = n_{total}/V_{specimen} = N_v$.

For the two-layer case (one microcracked layer and one undamaged layer), the equation for the relative Young's modulus change becomes

$$\frac{E_s - \bar{E}_{2_{ROM}}}{E_s} = v_\ell fG_\ell N_\ell = \frac{a}{a+1} fG_\ell N_\ell = fG_\ell N_v \quad (8)$$

where a is d_ℓ/d_s and thus $v_\ell = a/(a+1)$. In Fig. 3 the fractional modulus change, $(E_s - \bar{E}_{2_{ROM}})/E_s$, is plotted as a function of a and N_ℓ (Equation 8).

Thus, for the ROM model (Equations 7 and 8), the fractional Young's modulus change induced by microcracking, $(E_s - E)/E_s$, can be expressed as a linear function of the microcrack volume number density N_v and the crack geometry factor G. (In order to obtain Equation 7, we considered the special case where the alignment factor f and the geometry factor G were identical for the two microcracked layers.) Equations 7 and 8 are equivalent to Equation 1, in which the microcracks are distributed over the entire specimen volume. This result implies that in the two-layer and three-layer composite ROM models (Equations 7, 8, and Appendix A), non-interacting crack populations have the same effect on modulus decrement whether the cracks are confined within a surface layer(s) or whether the crack centroids are distributed homogeneously within the specimen. Physically, this result can be understood within the context of the ROM model itself (Appendix A). For a surface-microcracked specimen loaded in uniaxial tension, where the loading axis is normal to the microcracked surfaces (Fig. A1a and b in Appendix A), the modulus of the specimen will be unaffected whether the microcracks remain constrained to the microcracked surface layer or whether the microcracks are allowed to "float" in directions parallel to the crack faces and take on positions where the crack centroids are (on average) homogeneously distributed throughout the volume of the specimen.

We shall now express the fractional changes in Young's modulus in the three-layer (Equation 6) and two-layer (Equation 8) ROM models in terms of the thickness of microcrack-damaged layers. This will allow us to more directly compare this section's ROM results with the dynamic modulus expressions that will be developed in section 2.2. For both the ROM and dynamic modulus expressions, we express the results in terms of a relative geometry (thickness) of microcracked layer(s) and in terms of crack damage parameters (such as the crack orientation function f, the crack geometry function G and the crack number density). Therefore, we can plot the relative modulus changes in terms of layer geometry and microcrack parameters, as shown schematically in Fig. 4a and b, respectively.

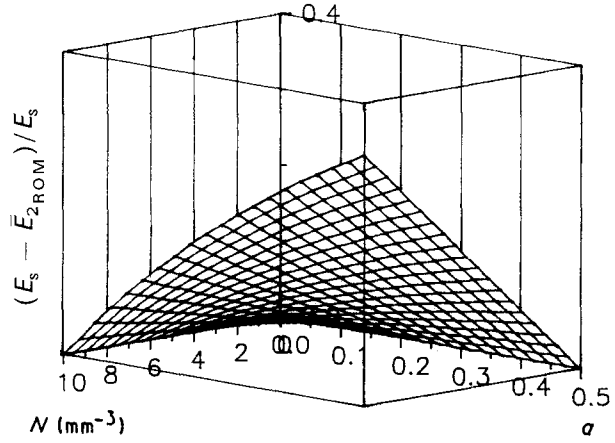

Figure 3 Relationship between crack number density N, relative damage-layer thickness a, and fractional modulus change for a two-layer composite based on the rule-of-mixtures model.

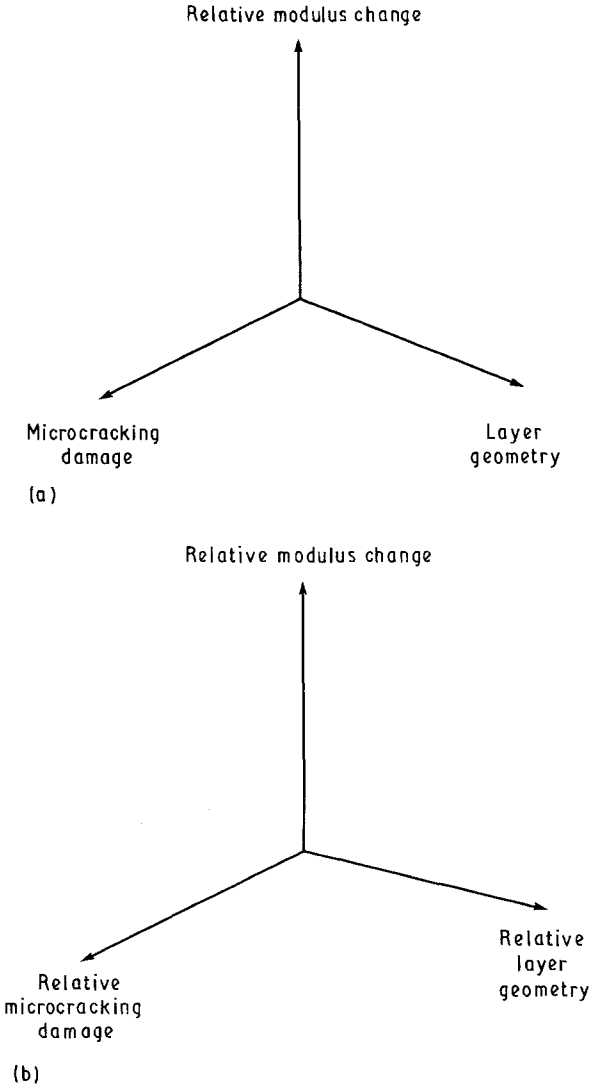

Figure 4 Schema for representing the relative modulus changes for (a) two-layer composite model and (b) three-layer composite model in terms of layer geometry and microcrack parameters.

If we label layer thicknesses as

$d_{\ell 1}$ = thickness of microcracked layer 1

$d_{\ell 2}$ = thickness of microcracked layer 2

d_s = thickness of the undamaged layer

and the relative layer thickness as $R_1 = d_{\ell 1}/d_s$, $R_2 = d_{\ell 2}/d_s$, then using Equation 6, $\bar{E}_{3_{ROM}}$ can be expressed as

$$\frac{E_s - \bar{E}_{3_{ROM}}}{E_s} = \frac{f_1 G_{\ell 1} N_{\ell 1} R_1 + f_2 G_{\ell 2} N_{\ell 2} R_2}{R_1 + R_2 + 1}$$

$$= \frac{R_1 \Lambda_1 + R_2 \Lambda_2}{R_1 + R_2 + 1} \quad (9a)$$

$$= \frac{\Lambda_2 d_{\ell 2}}{t}\left[\frac{d_{\ell 1}}{d_{\ell 2}}\left(\frac{\Lambda_1}{\Lambda_2}\right) + 1\right] \quad (9b)$$

$(E_s - \bar{E}_{3_{ROM}})/E_s$ thus can be written as a function of four variables R_1, Λ_1, R_2 and Λ_2 (Equation 9a) where $\Lambda_1 = f_1 G_{\ell 1} N_{\ell 1}$ and $\Lambda_2 = F_2 G_{\ell 2} N_{\ell 2}$. In order to plot the fractional modulus change function $(E_s - \bar{E}_{3_{ROM}})/E_s$ in a three-dimensional coordinate system (Fig. 5a) we use Equation 9b, which expresses the fractional modulus change as a function of the dimensionless variables Λ_1/Λ_2 and $d_{\ell 1}/d_{\ell 2}$ which from the definitions of R_1 and R_2, $d_{\ell 1}/d_{\ell 2}$ is equivalent to R_1/R_2.

If the crack geometry (shape and size) and crack alignment are the same for layers 1 and 2, then

$$\frac{E_s - \bar{E}_{3_{ROM}}}{E_s} = f G_\ell \frac{N_{\ell 1} R_1 + N_{\ell 2} R_2}{R_1 + R_2 + 1} \quad (10)$$

For the two-layer case (one microcracked layer and one undamaged layer), the equation for the relative Young's modulus change becomes

$$\frac{E_s - \bar{E}_{2_{ROM}}}{E_s} = \frac{a}{a+1} f G_\ell N_\ell = \frac{a}{a+1}\Lambda \quad (11)$$

where $a = d_\ell/d_s$ and $\Lambda = f G_\ell N_\ell$ (Fig. 5b).

2.2. Dynamic beam vibration model

2.2.1. Two-layer dynamic beam vibration model

The overall Young's modulus of surface-microcracked specimens can be predicted using a dynamic beam vibration theory assuming a two-layer composite for specimens microcracked on a single surface (Fig. 1 and Appendix B):

$$\bar{E}_{2_{DYN}} = E_\ell \frac{I_\ell}{I_\ell + I_s} + E_s \frac{I_s}{I_\ell + I_s} \quad (12)$$

In Appendix B we show that the second moments of inertia I_s and I_ℓ are given by

$$I_s = \left(\frac{d_s^3}{3} - d_s^2 d + d_s d^2\right) w \quad (13a)$$

$$I_\ell = \left(\frac{d_\ell^3}{3} + d_\ell^2 d + d_\ell d^2\right) w \quad (13b)$$

where w = width of the specimen, d_ℓ = thickness of microcracked layer and d_s = thickness of undamaged layer. The neutral plane (Figs 1 and B1) is given (Equation B9, Appendix B) by

$$d = \frac{E_s d_s^2 - E_\ell d_\ell^2}{2E_s d_s + 2E_\ell d_\ell} \quad (14)$$

where E_ℓ = modulus of the microcracked layer and

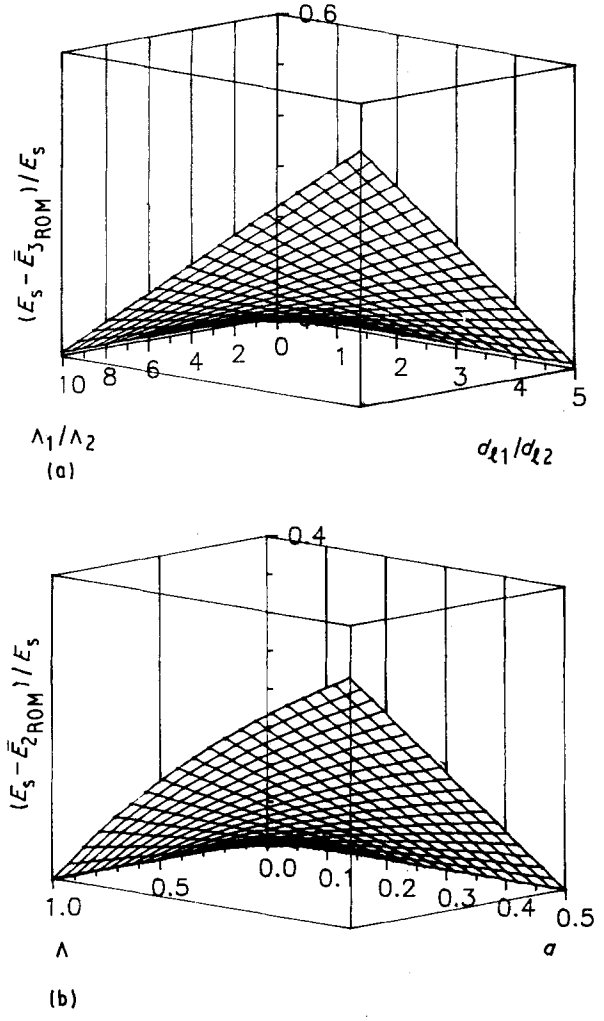

Figure 5 (a) Relation between $d_{\ell 1}/d_{\ell 2}$, Λ_1/Λ_2 ($\Lambda_1/\Lambda_2 = f_1 G_{\ell 1} N_{\ell 1}/f_1 G_{\ell 1} N_{\ell 1}$), and the fractional Young's modulus change for a three-layer composite based on rule-of-mixtures model (when $\Lambda_2 = 0.1$, $d_{\ell 2} = 0.1 \times$ bar thickness). (b) Relationship between a, Λ ($\Lambda = f G_\ell N_\ell$) and the fractional Young's modulus change for a two-layer composite based on rule-of-mixtures model.

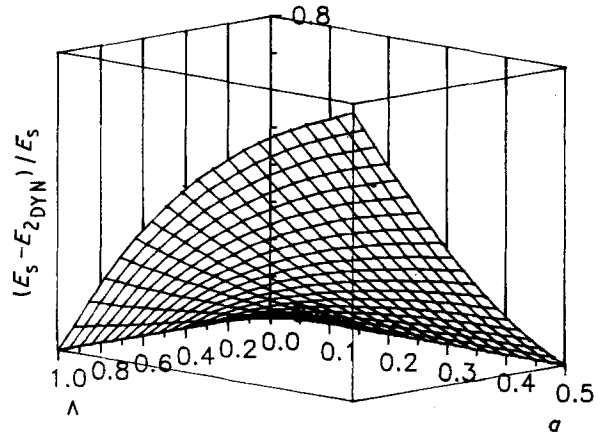

Figure 6 Relationship between a, Λ ($\Lambda = f G_\ell N_\ell$) and fractional Young's modulus change for a two-layer composite based on dynamic beam vibration model.

E_s = undamaged layer modulus. Using Equation 1, the modulus of the microcracked layer, E_ℓ, can be expressed in terms of the modulus of the undamaged layer E_s, the crack alignment function f, geometry factor G_ℓ, and the number density of cracks in the microcracked layer, N_ℓ, such that

$$E_\ell = E_s(1 - fG_\ell N_\ell) \tag{15}$$

Using Equations 12–15, the change in dynamic modulus due to microcracking in a two-layer composite (one microcrack-damaged layer and one undamaged layer) can be expressed as

$$\frac{E_s - \bar{E}_{2_{DYN}}}{E_s} = \Lambda \frac{I_\ell}{I_\ell + I_s}$$

$$= \frac{\Lambda[E_s^2 d_s^2 d_\ell(4d_\ell^2 + 6d_s d_\ell + 3d_s^2) + 2E_s E_\ell d_s d_\ell^4 + E_\ell^2 d_\ell^5]}{E_s^2 d_s^5 + 2E_s E_\ell d_s^4 d_\ell + E_\ell^2 d_s d_\ell^2(4d_s^2 + 6d_s d_\ell + 3d_\ell^2) + E_s^2 d_s^2 d_\ell(4d_\ell^2 + 6d_s d_\ell + 3d_s^2) + 2E_s E_\ell d_s d_\ell^4 + E_\ell^2 d_\ell^5} \tag{16}$$

Fig. 6 is a plot of Equation 16 in terms of a (where $a = d_\ell/d_s$) and the microcrack damage parameter Λ. Equation 16 is quite cumbersome and hence difficult to directly compare with the ROM results. Other than in a plot such as Fig. 6, the cumbersome nature of Equation 16 also make it difficult to readily observe the dependence of the relative modulus change upon the various parameters of moduli, layer thickness, etc. We shall thus derive a simplified (but approximate) form of Equation 16 which is more tractable to use for comparison with the ROM results and to display the functional dependencies on layer geometry and microcracking parameters.

Using Equation 15 and the relation $ad_s = d_\ell$, Equation 14 may be rewritten as

$$\bar{E}_{2_{DYN}} = \frac{E_s[(1 + a)^3 - (a^3 + a^2 + 3a + 3)C_2 - 6(1 + a)C_2^2]}{(1 + a)^3} \tag{26}$$

$$d = \frac{d_s^2[1 - (1 - \Lambda)a^2]}{2[1 + (1 - \Lambda)a]}$$

where $\Lambda = fG_\ell N_\ell$. Inserting Equation 15 into Equation 14 gives

$$d = \frac{d_s^2 - d_\ell^2 + d_\ell C_1}{2(d_s + d_\ell - C_1)} \tag{17}$$

where

$$C_1 = d_\ell f G_\ell N_\ell = fG_\ell N_A, \tag{18}$$

N_A = number density of cracks per unit area, $d_\ell + d_s = t$ = thickness of two-layer composite model and $d_s^2 - d_\ell^2 = (d_s + d_\ell)(d_s - d_\ell) = td_s - td_\ell$. Thus Equation 17 becomes

$$d = \frac{d_s}{2(1 - C_2)} - \frac{d_\ell}{2} \tag{19}$$

where

$$C_2 = \frac{C_1}{t} = \frac{d_\ell f G_\ell N_\ell}{t} = \frac{fG_\ell N_A}{t} = fG_\ell N_V \tag{20}$$

and N_V = volume crack number density, based on the volume of the entire specimen. To simplify our notation, we define $\beta = 1/(1 - C_2)$. Then Equation 19 becomes

$$d = \frac{\beta d_s - d_\ell}{2} \tag{21}$$

Inserting Equation 21 into Equation 13a and using the relation $a = d_\ell/d_s$ gives

$$I_s = \frac{d_s^3[4 - 6\beta + 3\beta^2 + 6(1 - \beta)a + 3a^2]w}{12} \tag{22}$$

When C_2 is small, $\beta = 1/(1 - C_2) \approx 1 + C_2$ and $C_2^2 \approx 0$. Then Equation 22 becomes

$$I_s = \frac{d_s^3(1 + 3a^2 - 6aC_2)w}{12} \tag{23}$$

Inserting Equation 21 into Equation 13a gives

$$I_\ell = \frac{d_s^3(a^3 + 3a + 6aC_2)w}{12} \tag{24}$$

Combining terms in Equations 23 and 24 yields

$$I_s + I_\ell = \frac{d_s^3(1 + a)^3 w}{12} \tag{25}$$

Inserting Equations 16 and 23–25 into Equation 12 gives

Neglecting terms of order C_2^2 gives

$$\frac{E_s - \bar{E}_{2_{DYN}}}{E_s} = \frac{a^2 + 3}{(a + 1)^2} v_\ell \Lambda = \frac{a(a^2 + 3)}{(a + 1)^3} \Lambda \tag{27}$$

where $a = d_\ell/d_s$ and $a/(a + 1) = d_\ell/t = v_\ell$. As a comparison with the ROM results (Equation 11) for the two-layer composite system, we can write

$$\frac{E_s - \bar{E}_{2_{DYN}}}{E_s} = \frac{a^2 + 3}{(a + 1)^2} \frac{E_s - \bar{E}_{2_{ROM}}}{E_s} = g(a) \frac{E_s - \bar{E}_{2_{ROM}}}{E_s} \tag{28}$$

where $g(a) = (a^2 + 3)/(a + 1)^2$ is a polynomial function of the relative layer geometry and $a = d_\ell/d_s$ (Fig. 1a shows d_ℓ and d_s). As $a \to 0$ the damage layer thickness $d_\ell \to 0$, which in turn means that C_2 approaches zero. When $C_2 \to 0$, $\bar{E}_{2_{DYN}}$ approaches the undamaged modulus E_s. For a finite layer thickness d_ℓ and a finite specimen thickness t, $C_2 \to 0$ implies that the microcrack damage ($fG_\ell N_\ell$) goes to zero, which is consistent with $E_{2_{DYN}} \to E_s$ (Equation 2d). When a approaches infinity, $\bar{E}_{2_{DYN}}$ becomes

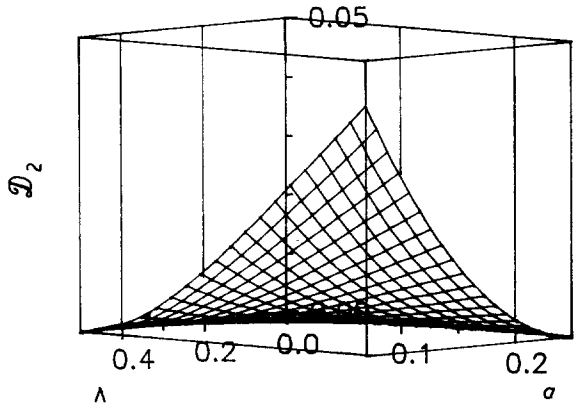

Figure 7 The difference $\mathscr{D}_2$ between the two-layer dynamic fractional modulus change (Equation 16) and its approximation (Equation 27) in terms of a and Λ.

$E_s(1 - fG_fN_V)$. Physically, as a becomes large, the layer thickness approaches the specimen thickness. As a approaches infinity, the layer thickness and the specimen thickness become the same, and thus the expression for $E_{2_{DYN}}$ becomes the same as Equation 1 for homogeneously microcracked materials (Appendix D).

The approximations given by Equations 27 and 28 (where Equations 27 and 28 are equivalent) give the fractional Young's modulus change due to surface-limited microcracking for a two-layer composite consisting of a microcracked layer and an undamaged layer (Fig. 1a). Equation 27 portrays the fractional Young's modulus change as a relatively simple function of a (the relative layer thickness) and Λ (the microcrack damage level), while Equation 28 allows one to compare the ROM and dynamic modulus models for the fractional Young's modulus change. The difference between the two-layer fractional modulus expression (Equation 16) and its approximation (Equation 27) is plotted as $\mathscr{D}_2$ on the vertical axis of Fig. 7. If the values of the relative layer thickness a and microcrack damage Λ are allowed to range independently over the interval [0, 0.1], then the maximum error due to the approximation (Equation 27) is about 2%. If a and Λ range independently over the intervals [0, 0.2] and [0, 0.3], then the maximum errors due to the approximation are about 7 and 14%, respectively. For values near the a or Λ axes (Figs 6 and 7), the errors tend to be low. For example for $a = 0.1$ and $\Lambda = 0.3$, the approximation error is about 5.5%, while at $a = 0.3$ and $\Lambda = 0.1$ the approximation error is about 6.3%. Note that for the ROM model, a figure similar to Fig. 7 is not needed, since the two-layer ROM fractional Young's modulus expression (Equation 11) is relatively straightforward and no further simplifying approximations are needed (as is the case for the dynamic modulus model) to make the equation manageable.

2.2.2. Three-layer dynamic beam vibration model

Equation 28 refers to a specimen microcracked on a single transverse face. For specimens microcracked on both long transverse surfaces (Fig. 1b), the overall Young's modulus of three-layer composites, $\bar{E}_{3_{DYN}}$, can be expressed in terms of dynamic beam vibration theory (Appendix B) such that

$$\bar{E}_{3_{DYN}} = E_{f1}\frac{I_{f1}}{I_{f1} + I_s + I_{f2}} + E_s\frac{I_s}{I_{f1} + I_s + I_{f2}} + E_{f2}\frac{I_{f2}}{I_{f1} + I_s + I_{f2}} \quad (29)$$

where

$$I_{f1} = \left((d_s - d)^2 d_{f1} + (d_s - d)d_{f1}^2 + \frac{d_{f1}^3}{3}\right)w \quad (30)$$

$$I_s = \left(\frac{d_s^3}{3} - d_s^2 d + d_s d^2\right)w \quad (31)$$

$$I_{f2} = \left(\frac{d_{f2}^3}{3} + d_{f2}^2 d + d_{f2}d^2\right)w \quad (32)$$

$$d = \frac{E_{f1}d_{f1}^2 + 2E_{f1}d_{f1}d_s + E_s d_s^2 - E_{f2}d_{f2}^2}{2E_{f1}d_{f1} + 2E_s d_s + 2E_{f2}d_{f2}} \quad (33)$$

in which d = distance between neutral plane and the interface between microcracked layer 2 and undamaged layer (Figs 1 and B2), w = width of the specimen, E_{f1}, E_{f2} = modulus of microcracked layer 1 and 2, respectively, and d_{f1}, d_{f2} = thickness of microcracked layer 1 and 2, respectively.

As was the case for the three-layer ROM model, E_{f1} and E_{f2}, the moduli of microcracked layers 1 and 2, respectively, for the three-layer dynamic model can be expressed in terms of E_s, the modulus of the undamaged layer and the crack damage parameters Λ_1 and Λ_2 (Equations 4a and b). By analogy with the two-layer dynamic model (Equation 16), the fractional modulus for the three-layer dynamic model can be obtained by substituting Equations 30–33 and Equations 4a and b into Equation 29. The fractional change in Young's modulus, $(E_s - \bar{E}_{3_{DYN}})/E_s$, increases monotonically as a function of the relative damage Λ_1/Λ_2 increases and as d_{f1}/d_{f2} increases (Fig. 8). The explicit equation for $(E_s - \bar{E}_{3_{DYN}})/E_s$ is extremely unwieldy and will not be reproduced here (although the

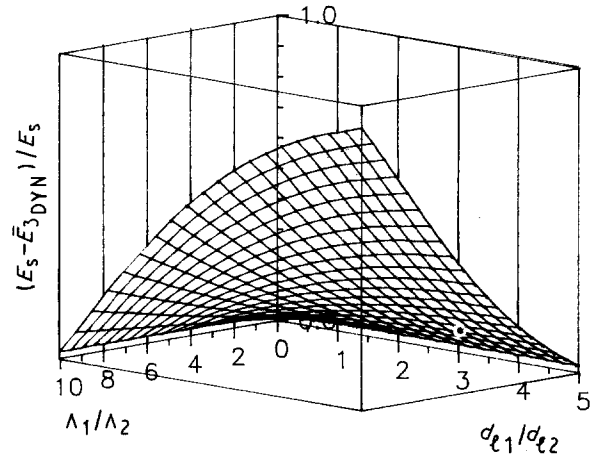

Figure 8 Relationship between d_{f1}/d_{f2}, Λ_1/Λ_2 and the fractional Young's modulus change for three-layer composite based on dynamic beam vibration model (when $\Lambda_2 = 0.1$, $d_{f2} = 0.1 \times$ bar thickness).

reader can readily produce it, if desired, via the substitutions listed above). However, as was the case for the two-layer dynamic model described by Equation 16, we can obtain an approximation for $(E_s - E_{3_{DYN}})/E_s$ which allows us to compare the three-layer dynamic model with the three-layer ROM results, which also gives simplified functional dependencies of the three-layer dynamic model on layer geometry and microcracking parameters.

We shall now derive an expression for small values of $\Lambda_1 v_1$ and $\Lambda_2 v_2$ analogous to the small-Λv expression obtained for the two-layer dynamic model (Equation 27). We begin by inserting into Equation 33 the expressions for E_{f1} and E_{f2} from Equations 4a and b to give

$$d = \frac{(1 - C_{b1})d_{f1} + (1 - 2C_{b1})d_s - (1 - C_{b2})d_{f2}}{2(1 - C_c)} \tag{34}$$

where

$$t = d_{f1} + d_s + d_{f2}$$

$$C_{b1} = \frac{f_1 G_{f1} N_{f1} d_{f1}}{t} = \frac{\Lambda_1 d_{f1}}{t} = \Lambda_1 v_1$$

$$C_{b2} = \frac{f_2 G_{f2} N_{f2} d_{f2}}{t} = \frac{\Lambda_2 d_{f2}}{t} = \Lambda_2 v_2$$

$$C_c = C_{b1} + C_{b2} = \Lambda_1 v_1 + \Lambda_2 v_2$$

For small C_c, $1/(1 - C_c) \approx 1 + C_c$. Dropping second-order terms in C_c gives

$$d = [1 + R_1 - R_2 - C_{b1}(1 + R_2) + C_{b2}(1 + R_1)]d_s/2 = Cd_s \tag{35}$$

where $R_1 = d_{f1}/d_s$, $R_2 = d_{f2}/d_s$ and

$$C = [1 + R_1 - R_2 - C_{b1}(1 + R_2) + C_{b2}(1 + R_1)]/2 \tag{36}$$

Thus the moments of inertia I_{f1}, I_s and I_{f2} can be expressed in terms of R_1, R_2, d_s and C:

$$I_{f1} = wd_s^3\left(\frac{R_1^3}{3} + (1 - C)R_1^2 + (1 - 2C + C^2)R_1\right) \tag{37}$$

$$I_s = wd_s^3(\tfrac{1}{3} - C + C^2) \tag{38}$$

$$I_{f2} = wd_s^3\left(\frac{R_2^3}{3} + CR_2^2 + C^2R_2\right) \tag{39}$$

If both C_{b1} and C_{b2} are small, then $C_{b1}^2 = C_{b2}^2 = C_{b1}C_{b2} \approx 0$ and thus

$$C^2 \approx (1 + R_1 - R_2)[1 + R_1 - R_2 - 2C_{b1}(1 + R_2) + 2C_{b2}(1 + R_1)/4] \tag{40}$$

After a bit of algebra, one obtains

$$\frac{E_s - \bar{E}_{3_{DYN}}}{E_s} = \frac{[R_1^2 + 3(R_2 + 1)^2]C_{b1} + [R_2^2 + 3(R_1 + 1)^2]C_{b2}}{(R_1 + R_2 + 1)^2} \tag{41a}$$

$$= \frac{R_1[R_1^2 + 3(R_2 + 1)^2]f_1 G_{f1} N_{f1} + R_2[R_2^2 + 3(R_1 + 1)^2]f_2 G_{f2} N_{f2}}{(R_1 + R_2 + 1)^3} \tag{41b}$$

where $R_1 = d_{f1}/d_s$, $R_2 = d_{f2}/d_s$. Thus the fractional decrease in Young's modulus for the three-layer dynamic modulus model can be written as

$$\frac{E_s - \bar{E}_{3_{DYN}}}{E_s} = g_1(R_1, R_2)f_1 G_{f1} N_{f1} + g_2(R_1, R_2)f_2 G_{f2} N_{f2} = g_1(R_1, R_2)\Lambda_1 + g_2(R_1, R_2)\Lambda_2 \tag{41c}$$

where $g_1(R_1, R_2)$ and $g_2(R_1, R_2)$ are the functions of relative layer geometry given in Equation 41b. If the damage layer thicknesses are equal, that is if $d_{f1} = d_{f2}$ and thus $R_1 = R_2 = a$ (Equation 36), then $g_1(R_1, R_2) = g_2(R_1, R_2) = g(a)$ such that Equation 41b becomes

$$\frac{E_s - \bar{E}_{3_{DYN}}}{E_s} = \frac{a(4a^2 + 6a + 3)}{(2a + 1)^3}(\Lambda_1 + \Lambda_2) = g(a)\frac{E_s - E_{3_{ROM}}}{E_s} \tag{42}$$

where $g(a) = (4a^2 + 6a + 3)/(2a + 1)^2$ and the fractional modulus change for the ROM model is given by Equation 10. Thus, for the three-layer dynamic modulus model, if $d_{f1} = d_{f2}$ then the fractional dynamic modulus change may be written as the product of a layer geometry factor $g(a)$ and the fractional ROM three-layer modulus change, by analogy with the two-layer expressions (Equation 28). However, in the general case that d_{f1} is not equal to d_{f2}, the layer geometry polynomials do not decouple, and the fractional changes in modulus cannot be expressed in terms of a simple multiple of $(E_s - \bar{E}_{3_{ROM}})/E_s$. The $\bar{E}_{3_{DYN}}$ values at various limits are given in Table 1.

Equations 41c and 42 (which are equivalent expressions) give approximations for the fractional Young's modulus change due to surface-limited microcracking for a three-layer composite consisting of two microcracked surface layers and an intervening undamaged layer (Fig. 1b). In addition to the comparison between the three-layer ROM model and dynamic modulus model given in Equation 42, Equation 41c expresses $(E_s - \bar{E}_{3_{DYN}})/E_s$ in terms of relative layer geometry functions, g_1 and g_2, and the microcrack damage parameters Λ_1 and Λ_2, As discussed above, the "full form" expression for $(E_s - \bar{E}_{3_{DYN}})/E_s$ may be obtained by substituting Equations 4a, 4b and 30–33 into Equation 29 (which gives a three-layer analogue of the two-layer model written explicitly as Equation 16). The difference between the 'full form" expression and its approximation (Equation 41c) is plotted as $\mathscr{D}_3$ on the vertical axis of Fig. 9. For the purpose of calculation we put Λ_2 at 0.1 and d_{f2} at $0.1t$, where t represents the thickness of the three-layer composite. As the values of the parameters d_{f1}/d_{f2} and Λ_1/Λ_2 range independently over the interval [0, 1], the max-

TABLE I $\bar{E}_{3DYN}$ values at various limiting values of the relative layer thicknesses R_1 and R_2

Conditions on R_1, R_2	$\bar{E}_{3DYN}$
$R_1 \to 0, R_2 \to 0$	E_s
$R_1 \to 0$	$E_s[1 - R_2(R_2^2 + 3)f_2 G_{f2} N_{f2}/(R_2 + 1)^3]$ the same as two-layer case (Equation 27)
$R_2 \to 0$	$E_s[1 - R_1(R_1^2 + 3)f_1 G_{f1} N_{f1}/(R_1 + 1)^3]$ the same as two-layer case (Equation 27)
$R_1 \to 0, R_2 \to \infty$	$E_s(1 - f_2 G_{f2} N_{f2})$ the same as the case of homogeneously distributed cracks throughout the body (Equation 1)
$R_1 \to \infty, R_2 \to 0$	$E_s(1 - f_1 G_{f1} N_{f1})$ the same as the case of homogeneously distributed cracks throughout the body (Equation 1)
$R_1 \to \infty, R_2 \to \infty$	$E_s\{1 - [\lambda(f_1 G_{f1} N_{f1} - f_2 G_{f2} N_{f2}) + f_2 G_{f2} N_{f2}]\}$ where $\lambda = 4[d_{f1}/(d_{f1} + d_{f2})]^3 - 6[d_{f1}/(d_{f1} + d_{f2})]^2 + 3d_{f1}/(d_{f1} + d_{f2})$ (see Appendix D)

imum error due to approximation (Equation 41c) is slightly less than 2%. As d_{f1}/d_{f2} and Λ_1/Λ_2 range independently over the intervals [0, 2] and [0, 3] then the maximum errors due to approximation are 3 and 10%, respectively. If d_{f1}/d_{f2} and Λ_1/Λ_2 are allowed to independently take on any value in the interval [0, 5], then the maximum error due to approximation is about 25%.

As in the case of the two-layer ROM model, a figure similar to Fig. 9 is not needed since the three-layer ROM fractional Young's modulus expression (Equation 6) can already be expressed straightforwardly in terms of the relative layer geometry parameters R_1 and R_2 and the microcrack damage parameters Λ_1 and Λ_2.

3. Comparison of ROM and dynamic modulus models

When the layer thickness d_f approaches zero for a two-layer composite ($a \to 0$), the ratio of fractional Young's modulus change (dynamic beam vibration theory, Equation 27) to fractional Young's modulus change (rule of mixtures, Equation 11) approaches 3 (Appendix C). When layer thickness d_f approaches the bar thickness for a two-layer composite ($a \to \infty$), the ratio $\mathscr{R}_2$ of fractional Young's modulus change (dynamic beam vibration theory, Equation 27) to fractional Young's modulus change (rule of mixtures, Equation 11) approaches unity (see Appendix C and Fig. 10a).

For the three-layer composite model, when the layer thicknesses d_{f1} and d_{f2} both approach zero (that is, for R_1 and $R_2 \to 0$) the ratio $\mathscr{R}_3$ of fractional modulus changes for the dynamic model (Equation 41b) and the ROM model (Equation 10) approaches 3 (see Appendix C and Fig. 10b).

For both the two-layer and the three-layer composites, note that the measured moduli themselves do not differ by a factor of 3; it is only the microcrack-induced modulus changes (that is, the relative sensitivity to microcrack damage) that differ by a factor of 3 between the ROM and dynamic modulus models (Fig. 9a and b). Physically, one would expect the dynamic modulus technique to be more sensitive to surface-limited microcracks, since the maximum absolute values of strain during a dynamic modulus measurement occur at the specimen's surface (Appendix B), while under uniaxial tension (which is appropriate for the ROM model, as outlined in Appendix A) the strain is uniform throughout the specimen. Also, the factor of 3 difference in "sensitivity" applies to very thin surface damage layers, and as the volume fraction of the microcracked layer decreases (for a fixed microcrack damage level) the microcrack-induced modulus change decreases. Thus, in practice the approach to the asymptotic factor of 3 for $\mathscr{R}_2$ and $\mathscr{R}_3$ in Fig. 10a and b, respectively, would depend on the lower experimental threshold for measuring modulus changes. The smaller the microcrack-induced modulus changes that could be experimentally determined, the closer one could approach to $\mathscr{R}_2$ or $\mathscr{R}_3$ values of 3.

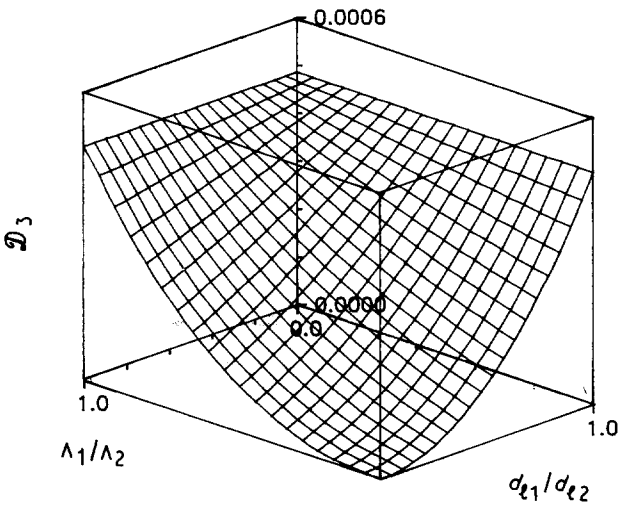

Figure 9 The difference $\mathscr{D}_3$ between the three-layer dynamic modulus (Equation 29) and its approximation (Equation 41c) in terms of d_{f1}/d_{f2} and Λ_1/Λ_2.

4. Summary and conclusions

Dynamic modulus and rule of mixtures microcracking-modulus models were presented, based on the

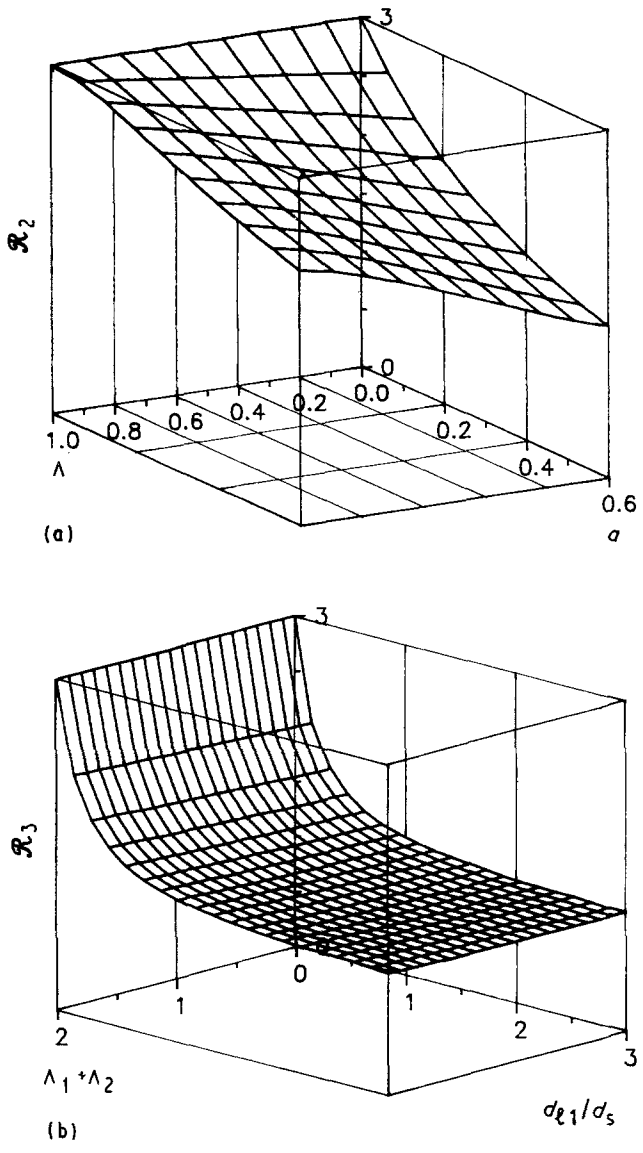

Figure 10 (a) Relationship between a, Λ and the ratio $\mathscr{R}_2$ of fractional Young's modulus change (dynamic) to fractional Young's modulus change (ROM) for two-layer composite. (b) Relationship between d_{f1}/d_s, $\Lambda_1 + \Lambda_2$ and the ratio $\mathscr{R}_3$ of fractional Young's modulus change (dynamic) to fractional Young's modulus change (ROM) for three-layer composite (when $d_{f1} = d_{f2}$, $\Lambda_1 = \Lambda_2$).

concept that a specimen containing a surface-limited population of microcracks could be viewed as a composite, with the microcrack-damaged regions as layers of reduced modulus ideally bonded to an undamaged layer.

In general, fractional modulus changes can thus be expressed in terms of a relative layer geometry and the crack damage parameter Λ which involves microcrack geometry, orientation and crack number density (as shown schematically in Fig. 4).

The fractional modulus change for the ROM model was given by Equations 8 and 11 in terms of a two-layer composite (one microcracked layer and one microcrack-free layer) and by Equations 6 and 9 for a three-layer composite (two microcracked surface layers that sandwich an intermediate microcrack-free layer). Since the fractional modulus changes for the dynamic modulus model are somewhat unwieldy (see Equation 16 for the two-layer case), approximations for the two-layer case (Equation 27) and the three-layer case (Equation 41c) were derived.

These simplified, approximate forms (Equations 27 and 41c) straightforwardly display the dependence of the fractional modulus change upon the relative geometry (thickness) of the microcracked surface layers and upon the crack damage parameter Λ. The errors due to approximation were then specified as a function of the layer geometry and microcrack parameters, where in general it is shown that the approximations are useful in the small $a\Lambda$ regime.

For a fixed level of microcrack damage severity and for a fixed microcracked surface layer depth, the dynamic modulus shows a greater sensitivity to the fractional modulus change than does the ROM model (Fig. 10a and b). This relative sensitivity, defined as $\mathscr{R}_2$ and $\mathscr{R}_3$ for the two-layer and three-layer composite models, respectively (section 3), depends on the relative layer thickness. For thick layers $\mathscr{R}_2$ and $\mathscr{R}_3$ approach unity, while for vanishingly thin layers $\mathscr{R}_2$ and $\mathscr{R}_3$ each approach 3 (Appendices C and D). These sensitivity differences are likely to be related to the uniaxial loading assumed by the ROM model (Appendix A) and to the beam vibration assumed by the dynamic modulus model used in this paper (Appendix B). For uniaxial loading the strains are uniform through the specimen, while in beam vibration the maximal strains occur near the specimen's surfaces. Physically, the greater sensitivity to microcracking-induced modulus changes occurs for the dynamic modulus case in which the greatest strains occur at the specimen surface, where the microcracked layers are located.

Except for the approximate forms (Equations 27 and 41c), each of the fractional modulus change expressions developed in this paper applies to an arbitrary relative layer thickness (for either one or two microcracked layers) and to an arbitrary microcrack damage state, as long as the damage can be expressed in terms of Equation 1. In the models presented here, the undamaged state of each of the specimen layers had the same modulus E_s (Equations 4a, 4b and 15), as is appropriate for a polycrystalline specimen in which surface microcrack populations are induced. However, the models presented in this paper could easily be extended to a microcracked laminate in which the layers are composed of dissimilar materials by assuming different values of microcrack-free moduli for each of the specimen's layers.

Part II [28] discusses various microcracking–modulus theories that may be expressed in terms of Equation 1. In addition, Part II considers some crack geometries not normally considered in microcracking-modulus theories, including indentation cracks which have a ligament (plastically deformed zone) joining the adjacent faces of the indentation cracks [28]. Part III [29] compares the results of the models developed in Parts I and II with experimental results obtained on indentation crack fields induced in a series of polycrystalline alumina specimens.

Appendix A: A rule-of-mixtures model for two-layer and three-layer composite models of surface-microcracked specimens

This appendix reviews a typical ROM model for the overall elastic modulus of a layered composite body [30]. Equations A6 and A9, which are the principal results of this appendix, are the starting points for the development of our ROM–modulus decrement model for the two-layer and three-layer cases, respectively. (Equations A6 and A9 correspond to Equations 2 and 3, respectively, in section 2.1). The purpose of this appendix is to highlight the assumptions involved in ROM models and thereby point out possible limitations and applications of such models.

For a two-layer composite (Fig. A1a) loaded in uniaxial tension, the relative value of the strains in the composite are [30]

$$e_{\text{layer}} = e_{\text{undamaged}} = e_{\text{overall}} \tag{A1}$$

where e_{layer} = strain in microcracked layer, $e_{\text{undamaged}}$ = strain in undamaged layer and e_{overall} = overall strain. The stresses in the microcracked layer (σ_f) and the undamaged layer (σ_s), respectively, are given by

$$\sigma_f = E_f e_f \tag{A2a}$$

$$\sigma_s = E_s e_s \tag{A2b}$$

For a microcracked layer of cross-sectional area A_f and an undamaged layer of cross-sectional area A_s, the load (force) P_f in the microcracked layer and the load P_s in the undamaged layer are given by

$$P_f = \sigma_f A_f = E_f e_f A_f \tag{A3a}$$

$$P_s = \sigma_s A_s = E_s e_s A_s \tag{A3b}$$

If $P_{\text{overall}} = P_f + P_s$ and $A_{\text{overall}} = A_f + A_s$ then $P_{\text{overall}} = \sigma_{\text{overall}} A_{\text{overall}} = \sigma_f A_f + \sigma_s A_s$, such that

$$\sigma_{\text{overall}} = \frac{\sigma_f A_f}{A_{\text{overall}}} + \frac{\sigma_s A_s}{A_{\text{overall}}} = \sigma_f v_f + \sigma_s v_s \tag{A4}$$

where v_f is the volume fraction of the microcracked layer and v_s is the volume fraction of the undamaged layer. Differentiation of Equation A4 with respect to strain results in [30]

$$\frac{d\sigma_{\text{overall}}}{de} = \left(\frac{d\sigma_f}{de}\right) v_f + \left(\frac{d\sigma_s}{de}\right) v_s \tag{A5}$$

If $d\sigma_f/de$ and $d\sigma_s/de$ are linear then $\bar{E}_{2_{\text{ROM}}}$, the effective overall modulus of the two-layer composite, is

$$\bar{E}_{2_{\text{ROM}}} = E_f v_f + E_s v_s \tag{A6}$$

For a three-layer composite (Fig. A1b), the strain in microcracked layer 1 = strain in microcracked layer 2 = strain in undamaged layer = overall strain such

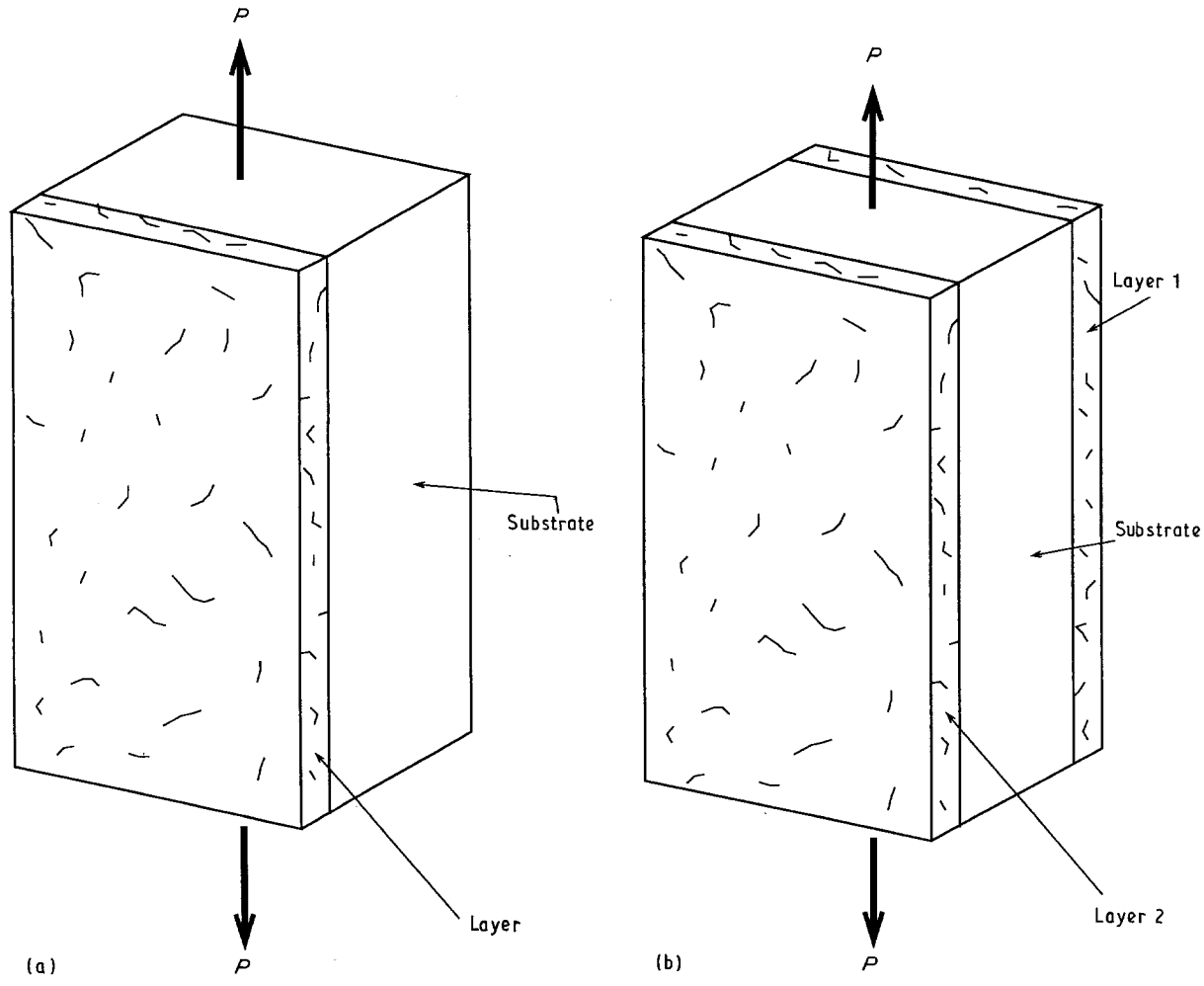

Figure A1 Schematic diagram of uniaxial tensile loading for (a) two-layer composite and (b) three-layer composite models.

that

$$e_{\text{layer 1}} = e_{\text{layer 2}} = e_{\text{undamaged}} = e_{\text{overall}} \quad \text{(A7)}$$

A procedure similar to that used for Equations A1–A5 (the two-layer composite case) yields the following three-layer expression [30]:

$$\frac{d\sigma_{\text{overall}}}{de} = \left(\frac{d\sigma_{\ell 1}}{de}\right)v_{\ell 1} + \left(\frac{d\sigma_s}{de}\right)v_s + \left(\frac{d\sigma_{\ell 2}}{de}\right)v_{\ell 2} \quad \text{(A8)}$$

where subscripts 1 and 2 refer to microcracked layers 1 and 2, respectively. If $d\sigma_{\ell 1}/de$, $d\sigma_{\ell 2}/de$ and $d\sigma_s/de$ are linear then

$$\bar{E}_{3\text{ROM}} = E_{\ell 1}v_{\ell 1} + E_s v_s + E_{\ell 2}v_{\ell 2} \quad \text{(A9)}$$

If the stress–strain behaviour for the non-microcracked ceramic is linear (which is typically true, except at very high temperatures), then $d\sigma_s/de$ should be linear, since it refers to the non-microcracked stress–strain behaviour. A key assumption for the ROM model is then the linearity of $d\sigma_\ell/de$, which refers to the stress–strain behaviour of the microcracked layer(s). However, a limited non-linearity of the elastic modulus for some ceramics under thermal shock conditions has been recently proposed by Swain [31].

Appendix B: Layer composite model approach for Young's modulus change using dynamic beam vibration theory

The free, undamped vibration of a monolithic bar can be described approximately by the Bernoulli–Euler beam equation [32, 33]

$$EI\frac{\partial^4 W(x,t)}{\partial x^4} + \left(\frac{A\rho}{g}\right)\frac{\partial^2 W(x,t)}{\partial t^2} = 0 \quad \text{(B1)}$$

where E = Young's modulus, I = second moment of inertia of the cross-section of the bar with respect to the neutral axis, W = transverse deflection of the bar, which is a function of position along longitudinal axis x and time t, A = cross-sectional area of the bar, ρ = density of the bar and g = acceleration due to gravity. Assuming perfect interfacial bonding between the microcracked layer and the undamaged layer, for a single microcracked layer (Fig. B1) Equation B1 becomes [32]

$$(E_s I_s + E_\ell I_\ell)\frac{\partial^4 W(x,t)}{\partial x^4} + \frac{(A_\ell\rho_\ell + A_s\rho_s)}{g}\frac{\partial^2 W(x,t)}{\partial t^2} = 0 \quad \text{(B2)}$$

where subscripts ℓ and s represent properties associated with the microcracked layer and undamaged layer, respectively. Since the change in the density due to microcracking typically is negligible and the sum of the microcracked layer cross-sectional area and the undamaged layer area is the total cross-sectional area of the beam, $(A_\ell\rho_\ell + A_s\rho_s)/g$ in Equation B2 can be approximated by $A\rho/g$.

The transverse vibration of a bar for free-free suspension requires that the bending moments and the shearing forces be zero at both ends of the bar

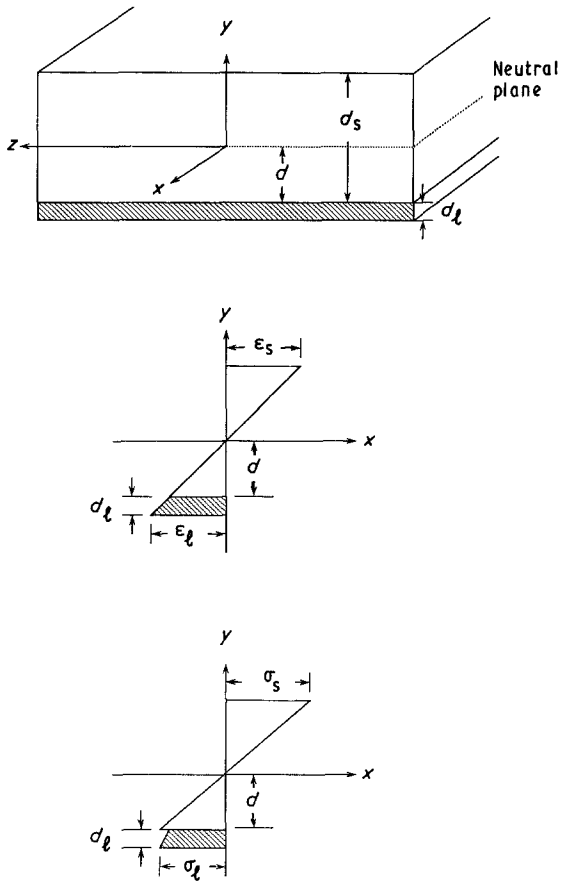

Figure B1 Schematic diagram of two-layer model composite beam showing the strain and stress distributions.

[32–34], such that

$$\frac{\partial^2 W(0,t)}{\partial x^2} = 0 \qquad \frac{\partial^3 W(0,t)}{\partial x^3} = 0 \qquad \text{for } t \geqslant 0 \quad \text{(B3)}$$

$$\frac{\partial^2 W(L,t)}{\partial x^2} = 0 \qquad \frac{\partial^3 W(L,t)}{\partial x^3} = 0 \qquad \text{for } t \geqslant 0 \quad \text{(B4)}$$

where L = length of the specimen. The solution of Equation B2 under the boundary conditions given in Equations B3 and B4 gives [32–34] the fundamental transverse (flexural) vibration frequency F of the composite:

$$F = \frac{k_1^2}{2\pi}\left[\frac{(E_s I_s + E_\ell I_\ell)g}{A\rho}\right]^{1/2} = \frac{11.1528}{L^2} \times \left[\frac{(E_s I_s + E_\ell I_\ell)g}{A\rho}\right]^{1/2} \quad \text{(B5)}$$

The second moments of inertia I_s and I_ℓ (Fig. B1) are given by

$$I_s = \int_{-d}^{d_s - d} y^2 dA = \left[\frac{d_s^3}{3} - d_s^2 d + d_s d^2\right]w \quad \text{(B6a)}$$

$$I_\ell = \int_{-d-d_\ell}^{-d} y^2 dA = \left[\frac{d_\ell^3}{3} + d_\ell^2 d + d_\ell d^2\right]w \quad \text{(B6b)}$$

where w = width of specimen, d_ℓ = thickness of microcracked layer and d_s = thickness of undamaged layer.

When the two-layer composite beam (Fig. B1) experiences pure bending, the neutral axis of the beam shifts from the centroid of cross-section of the composite beam to the stiffer side. The distance from the neutral axis to the interface between the microcracked and the undamaged layers, d, can be calculated using the equilibrium of the axial forces generated during pure bending [35] (Fig. B1):

$$\int_{-d}^{d_s-d} \sigma_s \, dA + \int_{-d-d_\ell}^{-d} \sigma_\ell \, dA = 0 \qquad \text{(B7)}$$

where

σ_ℓ = normal stress of microcracked layer = $E_\ell y/r$ (B8a)

σ_s = normal stress of undamaged layer = $E_s y/r$ (B8b)

and r = radius of curvature of the neutral axis. Stresses σ_ℓ and σ_s can be expressed in terms of E_ℓ, E_s, d_ℓ and d_s such that using Equations B8a and B8b, the following expression for d may be obtained from Equation B7:

$$d = \frac{E_s d_s^2 - E_\ell d_\ell^2}{2E_s d_s + 2E_\ell d_\ell} \qquad \text{(B9)}$$

Substituting Equations B6–B9 into B5 gives the calculated fundamental transverse frequencies for a two-layer composite beam:

$$F = \frac{6.4391}{L^2}\left[\frac{[E_s d_s^3 + E_\ell d_\ell^3 - 3(E_s d_s^2 - E_\ell d_\ell^2)/4(E_s d_s + E_\ell d_\ell)]g}{(d_s + d_\ell)\rho}\right]^{1/2} \qquad \text{(B10)}$$

The overall Young's modulus, $\bar{E}_{2_{DYN}}$, for the two-layer composite model is thus given by

$$\bar{E}_{2_{DYN}} = \frac{E_\ell I_\ell + E_s I_s}{I_\ell + I_s} \qquad \text{(B11)}$$

For specimens microcracked on both long transverse faces (Figs 1b and 2 in the main text) a three-layer composite model applies in which an intermediate, undamaged layer is sandwiched between microcracked layers 1 and 2. Again assuming perfect interfacial bonding between the microcracked layers and the undamaged layer (Fig. B2), Equation B1 for the three-layer case becomes

$$(E_{\ell 1} I_{\ell 1} + E_s I_s + E_{\ell 2} I_{\ell 2}) \frac{\partial^4 W(x,t)}{\partial x^4} + \left(\frac{A\rho}{g}\right) \frac{\partial^2 W(x,t)}{\partial t^2} = 0 \qquad \text{(B12)}$$

where $E_{\ell 1}$ = Young's modulus of microcracked layer 1 and $E_{\ell 2}$ = Young's modulus of microcracked layer 2. Applying the free–free end boundary conditions (Equation B4) gives the fundamental transverse vibration frequency for a three-layer composite (Fig. B2):

$$F = \frac{11.1528}{L^2}\left(\frac{(E_{\ell 1} I_{\ell 1} + E_s I_s + E_{\ell 2} I_{\ell 2})g}{A\rho}\right)^{1/2} \qquad \text{(B13)}$$

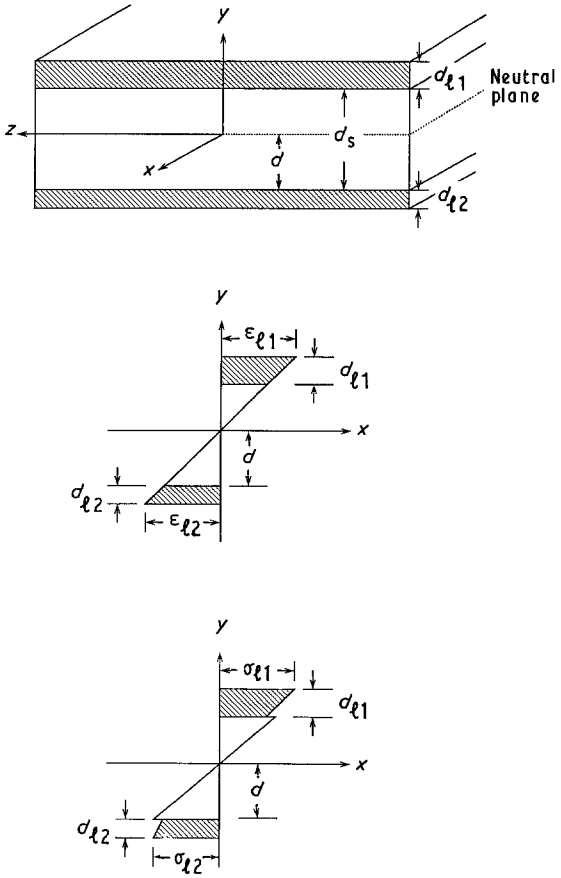

Figure B2 Schematic diagram of three-layer model composite beam showing the strain and stress distributions.

$$I_{\ell 1} = \int_{d_s-d}^{d_s+d_{\ell 1}-d} y^2 \, dA = \left[(d_s - d)^2 d_{\ell 1} + (d_s - d) d_{\ell 1}^2 + \frac{d_{\ell 1}^3}{3}\right] w \qquad \text{(B14a)}$$

$$I_s = \int_{-d}^{d_s-d} y^2 \, dA = \left[\frac{d_s^3}{3} - d_s^2 d + d_s d^2\right] w \qquad \text{(B14b)}$$

$$I_{\ell 2} = \int_{-d-d_{\ell 2}}^{-d} y^2 \, dA = \left[\frac{d_{\ell 2}^3}{3} + d_{\ell 2}^2 d + d_{\ell 2} d^2\right] w \qquad \text{(B14c)}$$

where $d_{\ell 1}$, $d_{\ell 2}$ = thickness of microcracked layer 1 and 2, respectively, d_s = thickness of undamaged layer and w = width of specimen. From the equilibrium of the axial forces (Fig. B2),

$$\int_{d_s-d}^{d_s+d_{\ell 1}-d} \sigma_{\ell 1} \, dA + \int_{-d}^{d_s-d} \sigma_s \, dA + \int_{-d-d_{\ell 2}}^{-d} \sigma_{\ell 2} \, dA = 0 \qquad \text{(B15)}$$

where

$\sigma_{\ell 1}$ = normal stress of microcracked layer 1 = $E_{\ell 1} y/r$ (B16a)

σ_s = normal stress of undamaged layer = $E_s y/r$ (B16b)

$$\sigma_{f2} = \text{normal stress of microcracked layer 2} = E_{f2}y/r \quad \text{(B16c)}$$

and r = radius of curvature of the neutral axis. The distance d from the neutral axis to the interface between microcracked layer 2 and the undamaged layer is calculated in terms of known values:

$$d = \frac{E_{f1}d_{f1}^2 + 2E_{f1}d_{f1}d_s + E_sd_{fs}^2 - E_{f2}d_{f2}^2}{2E_{f1}d_{f1} + 2E_sd_s + 2E_{f2}d_{f2}} \quad \text{(B17)}$$

Substituting Equations B15 and B18 into B14 allows one to calculate the fundamental transverse vibration frequency.

The overall Young's modulus $\bar{E}_{3_{DYN}}$ of a three-layer composite model is

$$\bar{E}_{3_{DYN}} = \frac{E_{f1}I_{f1} + E_sI_s + E_{f2}I_{f2}}{I_{f1} + I_s + I_{f2}} \quad \text{(B18)}$$

Appendix C: The ratio of fractional Young's modulus change (dynamic) to fractional Young's modulus change (ROM) when the relative microcracked layer thickness (d_f/d_s) approaches zero

For the two-layer composite model, the second moment of inertia of the microcracked layer (Equation 13b in the main text) can be written as the following when the relative layer thickness becomes small ($d_f \ll t$):

$$I_f \approx d_fd^2w \quad \text{(C1)}$$

When $d_f \ll t$, then $d_s \approx 2d$ (Fig. B1 in Appendix B). The moment of inertia of the undamaged layer (Equation 13a in main text) can be expressed as

$$I_s \approx 2d^3w/3 \quad \text{(C2)}$$

where d is in turn approximately one-half of the specimen thickness, t, when $d_f \ll t$. Physically, when the thickness of the microcracked layer becomes small, the specimen approaches the homogeneous, undamaged case where the neutral plane is located at the specimen's mid-plane. Thus Equations C1 and C2 become

$$I_f = d_ft^2w/4 \quad \text{(C3)}$$

$$I_s = t^3w/12 \quad \text{(C4)}$$

$$I_s + I_f = \frac{wt^3}{12}\left[1 + 3\left(\frac{d_f}{t}\right)\right] = I_s\left[1 + 3\left(\frac{d_f}{t}\right)\right] \quad \text{(C5)}$$

Using the second moments of inertia for the two-layer case (Fig. 1a), we express the differences between the undamaged elastic modulus E_s and the effective elastic moduli for the two-layer dynamic model ($\bar{E}_{2_{DYN}}$) as

$$E_s - \bar{E}_{2_{DYN}} = \frac{3(d_f/t)(E_s - E_f)}{1 + 3(d_f/t)} \approx 3\left(\frac{d_f}{t}\right)(E_s - E_f) \quad \text{(C6)}$$

For two-layer ROM model $\bar{E}_{2_{ROM}}$ we use the relations $v_s = 1 - (d_f/t)$ and $v_f = d_f/t$ along with Equation 2 to obtain

$$E_s - \bar{E}_{2_{ROM}} = E_s - E_s\left(1 - \frac{d_f}{t}\right) + \frac{E_fd_f}{t} = \frac{d_f}{t}(E_s - E_f) \quad \text{(C7)}$$

In the limit that the ratio $d_f/t \to 0$, the relative sensitivity of the dynamic model and the ROM models (for the two-layer case) is given by

$$\lim_{(d_f/t)\to 0}\left(\frac{E_s - \bar{E}_{2_{DYN}}}{E_s - \bar{E}_{2_{ROM}}}\right) = \lim_{(d_f/t)\to 0}\left(\frac{3(d_f/t)(E_s - E_f)}{(d_f/t)(E_s - E_f)}\right) = 3 \quad \text{(C8)}$$

According to Equation C8, in the limit of a vanishingly small relative thickness (d_f/t) for the microcracked layer, the dynamic modulus is three times more sensitive than the ROM modulus to the relative changes in elastic modulus induced by microcracking. Physically, Equation C8 reflects the fact that the dynamic model is a beam vibration model (Appendix B) in which the elastic modulus is related to the resonant frequency of the beam, while in contrast the ROM model (Appendix A) is based upon a specimen loaded in uniaxial tension. For beam vibration, the maximum tensile and compressive stresses appear at the outer fibre of the beam (Appendix B, and especially Figs B1 and B2), while in the ROM model the uniaxial tension is constant over the cross-section of the beam. In the limit of a very thin microcracked surface layer, the microcracks are subject to the highest stresses present in the beam, while in the ROM model the microcracks are subject to the average stress over the specimen cross-section. The asymptotic limit represented by Equation C8 may be seen in the R axis intercept in Fig. 10a (main text), where R refers to the ratio of the fractional modulus changes for the dynamic and ROM modulus models.

For the three-layer composite model, when $d_{f1} \ll t$ and $d_{f2} \ll t$ then the second moments of inertia (Equations 30–32 in main text) become (upon dropping second- and third-order terms in d_{f1} and d_{f2})

$$I_{f1} = (d_s - d)^2d_{f1}w \quad \text{(C9)}$$

$$I_s = \left(\frac{d_s^3}{3} - d_s^2d + d_sd^2\right)w \quad \text{(C10)}$$

$$I_{f2} = d_{f2}d^2w \quad \text{(C11)}$$

$d_s \approx t \approx 2d$ when $d_{f1} \to 0$ and $d_{f2} \to 0$. Thus Equations C9–C11 become

$$I_{f1} = t^2d_{f1}w/4 = 3I_sd_{f1}/t \quad \text{(C12)}$$

$$I_s = t^3w/12 \quad \text{(C13)}$$

$$I_{f2} = t^2d_{f2}w/4 = 3I_sd_{f2}/t \quad \text{(C14)}$$

so that

$$I_{f1} + I_s + I_{f2} = I_s\left[3\left(\frac{d_{f1}}{t}\right) + 1 + 3\left(\frac{d_{f2}}{t}\right)\right] \quad \text{(C15)}$$

Thus, from Equations C12–C15 and Equation 29 of

the main text

$$E_s - \bar{E}_{3_{DYN}} = \frac{-3(d_{f1}/t)E_{f1} + 3(d_{f1}/t)E_s + 3(d_{f2}/t)E_s - 3(d_{f2}/t)E_{f2}}{3(d_{f1}/t) + 1 + 3(d_{f2}/t)}$$

$$\approx -3\left(\frac{d_{f1}}{t}\right)E_{f1} + 3\left(\frac{d_{f1}}{t}\right)E_s + 3\left(\frac{d_{f2}}{t}\right)E_s - 3\left(\frac{d_{f2}}{t}\right)E_{f2} \quad \text{(C16)}$$

From Equation 3 of the main text we obtain

$$E_s - \bar{E}_{3_{ROM}} = -\frac{d_{f1}}{t}E_{f1} + \frac{d_{f1}}{t}E_s + \frac{d_{f2}}{t}E_s - \frac{d_{f2}}{t}E_{f2} \quad \text{(C17)}$$

Thus, in the limit the expression for the three-layer case becomes

$$\lim_{(d_f/t)\to 0}\left(\frac{E_s - \bar{E}_{3_{DYN}}}{E_s - \bar{E}_{3_{ROM}}}\right) = \lim_{(d_f/t)\to 0}\left[\frac{E_s - \bar{E}_{3_{DYN}}}{E_s}\left(\frac{E_s}{E_s - \bar{E}_{3_{ROM}}}\right)\right]$$

$$= \lim_{(d_f/t)\to 0}\left(\frac{3[-(d_{f1}/t)E_{f1} + (d_{f1}/t)E_s + (d_{f2}/t)E_s - (d_{f2}/t)E_{f2}]}{-(d_{f1}/t)E_{f1} + (d_{f1}/t)E_s + (d_{f2}/t)E_s - (d_{f2}/t)E_{f2}}\right) = 3 \quad \text{(C18)}$$

Thus for both the two-layer model (Equation C8) and the three-layer one (Equation C18), the fractional overall Young's modulus change (dynamic beam vibration theory) is three times larger than the fractional Young's modulus change (rule of mixtures) when the layer thickness is very thin compared with the undamaged layer thickness ($d_{f1} \to 0$ and $d_{f2} \to 0$).

Appendix D: Limiting values of $(E_s - \bar{E}_{3_{DYN}})/E_s$ and $(E_s - \bar{E}_{3_{ROM}})/E_s$ for the case that the microcrack volume dominates the specimen volume ($d_s \to 0$)

Using $\Lambda_1 = f_1 G_{f1} N_{f1}$ and $\Lambda_2 = f_2 G_{f2} N_{f2}$, Equation 41b of the main text may be rewritten as

$$\frac{E_s - \bar{E}_{3_{DYN}}}{E_s} = \frac{R_1[R_1^2 + 3(R_2+1)^2]\Lambda_1 + R_2[R_2^2 + 3(R_1+1)^2]\Lambda_2}{(R_1 + R_2 + 1)^3}$$

$$= \frac{d_{f1}[d_{f1}^2 + 3(d_{f2} + d_s)^2]\Lambda_1 + d_{f2}[d_{f2}^2 + 3(d_{f1} + d_s)^2]\Lambda_2}{t^3} \quad \text{(D1)}$$

where d_{f1} = thickness of microcracked layer 1, d_{f2} = thickness of microcracked layer 2, d_s = thickness of undamaged layer, $t = d_{f1} + d_s + d_{f2}$ (specimen thickness) and $R_1 = d_{f1}/d_s$, $R_2 = d_{f2}/d_s$. If $R_1 \to \infty$ or $R_2 \to \infty$ or equivalently if either $d_{f1} \to t$ or $d_{f2} \to t$ (Fig. D1), then for the dynamic three-layer model

$$\lim_{d_s\to 0}\left(\frac{E_s - \bar{E}_{3_{DYN}}}{E_s}\right) = \frac{d_{f1}(d_{f1}^2 + 3d_{f2}^2)\Lambda_1 + d_{f2}(d_{f2}^2 + 3d_{f1}^2)\Lambda_2}{t^3}$$

$$= \left[\left(\frac{d_{f1}}{t}\right)^3 + 3\left(\frac{d_{f2}^2 d_{f1}}{t^3}\right)\right]\Lambda_1 + \left[\left(\frac{d_{f2}}{t}\right)^3 + 3\left(\frac{d_{f1}^2 d_{f2}}{t^3}\right)\right]\Lambda_2 \quad \text{(D2a)}$$

or

$$\lim_{d_s\to 0}\left(\frac{E_s - \bar{E}_{3_{DYN}}}{E_s}\right) = (v_1^3 + 3v_2^2 v_1)\Lambda_1 + (v_2^3 + 3v_1^2 v_2)\Lambda_2$$

$$= \Lambda_2\left\{\left[\left(\frac{d_{f1}}{d_{f2}}\right)^3 + 3\left(\frac{d_{f1}}{d_{f2}}\right)\right]\frac{\Lambda_1}{\Lambda_2} + \left[1 + 3\left(\frac{d_{f1}}{d_{f2}}\right)^2\right]\right\} \quad \text{(D2b)}$$

(see Fig. D2) where v_1, v_2 = volume fraction of microcracked layer 1 and 2, respectively, and d_{f1}, d_{f2} = thickness of microcracked layer 1 and 2, respectively. However, as $d_s \to 0$, $v_1 + v_2 = 1$ or $v_2 = 1 - v_1$. Thus Equation D2 may be rewritten in terms of volume fraction v_1 only such that

$$\lim_{d_s\to 0}\left(\frac{E_s - \bar{E}_{3_{DYN}}}{E_s}\right) = (4v_1^3 - 6v_1^2 + 3v_1)\Lambda_1 + (-4v_1^3 + 6v_1^2 - 3v_1 + 1)\Lambda_2 \quad \text{(D3)}$$

$$= \lambda(\Lambda_1 - \Lambda_2) + \Lambda_2$$

where $\lambda = 4v_1^3 - 6v_1^2 + 3v_1$. In the special case that $d_{f1} = d_{f2}$, then $v_1 = 0.5$ and $\lambda = 0.5$, and thus

$$\lim_{d_s\to 0}\left(\frac{E_s - \bar{E}_{3_{DYN}}}{E_s}\right) = \frac{\Lambda_1 + \Lambda_2}{2} \quad \text{(D4)}$$

For the ROM three-layer model, when $d_s \to 0$ then

$$\frac{E_s - E_{3_{ROM}}}{E_s} = \frac{R_1\Lambda_1}{R_1 + R_2 + 1} + \frac{R_2\Lambda_2}{R_1 + R_2 + 1}$$

$$= v_1(\Lambda_1 - \Lambda_2) + \Lambda_2. \quad \text{(D5)}$$

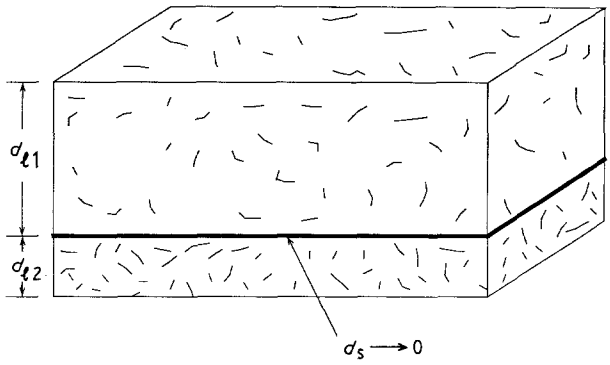

Figure D1 Schematic diagram of limiting case where the two microcracked layers dominate the specimen volume ($R_1 \rightarrow \infty$ and $R_2 \rightarrow \infty$).

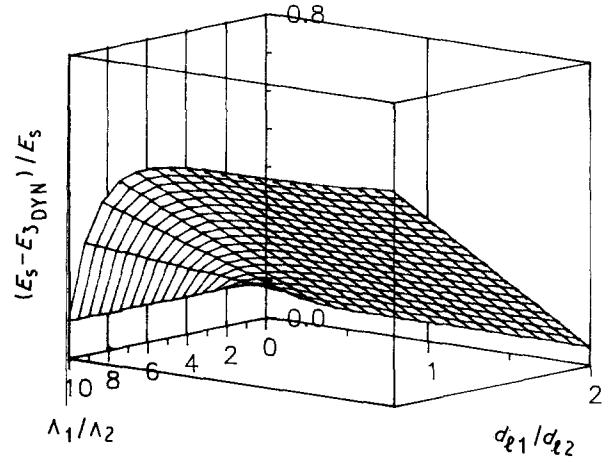

Figure D2 The relationship between $d_{\ell 1}/d_{\ell 2}$, Λ_1/Λ_2 and the limit of fractional Young's modulus change when both R_1 and R_2 go to infinity for three-layer model (for the particular case that $d_{\ell 2} = 0.1 \times$ bar thickness, $\Lambda_2 = 0.1$).

If $v_1 = 0.5$ (that is for $d_s \rightarrow 0$ and $d_{\ell 1} = d_{\ell 2}$) then

$$\lim_{d_s \rightarrow 0} \left(\frac{E_s - E_{3_{ROM}}}{E_s} \right) = \frac{\Lambda_1 + \Lambda_2}{2} \qquad \text{(D6)}$$

Thus the ROM result for the limit $v_1 = 0.5$ (Equation D6) is the same as the result obtained for the dynamic model when $v_1 = 0.5$ (Equation D4).

The ratio of the relative Young's modulus changes for the dynamic and ROM models can easily be obtained from the ratio of Equation D3 and D5 such that

$$\lim_{d_s \rightarrow 0} \left(\frac{E_s - E_{3_{DYN}}}{E_s - E_{3_{ROM}}} \right) = \frac{\lambda(\Lambda_1 - \Lambda_2) + \Lambda_2}{v_1(\Lambda_1 - \Lambda_2) + \Lambda_2} \qquad \text{(D7)}$$

In Equation D7, if $\Lambda_1 = \Lambda_2$ (where Λ_1 and Λ_2 measure the damage in microcracked layers 1 and 2) then for all values of v_1 (or v_2)

$$\lim_{d_s \rightarrow 0} \left(\frac{E_s - E_{3_{DYN}}}{E_s - E_{3_{ROM}}} \right) = 1 \qquad \text{(D8)}$$

Physically, for a vanishingly small undamaged layer ($d_s \rightarrow 0$), the condition that $\Lambda_1 = \Lambda_2$ implies that the effective damage in the two microcracked layers is identical, and thus the damage state approaches that of a uniformly microcracked body.

Now consider the general case that Λ_1 is not equal to Λ_2. If $v_1 \rightarrow 1$ (or equivalently if $v_2 \rightarrow 1$), or if $v_1 = v_2 = 0.5$, then the limit given by Equation D7 also approaches unity.

References

1. Y. KIM, W. J. LEE and E. D. CASE, in "Metal and Ceramic Matrix Composites: Processing, Modeling and Mechanical Behavior", edited by R. B. Bhagat, A. H. Clauer, P. Kumar and A. M. Ritter (Minerals, Metals and Materials Society, Warrendale, PA, 1990) pp. 479–486.
2. *Idem*, in Proceedings of 5th Technical Conference, June 12–14 1990, East Lansing, MI, American Society for Composites (Technonic Publishing Co, Lancaster PA 1990) pp. 871–881.
3. W. J. LEE and E. D. CASE, *Mater. Sci. Engng* **A119** (1989) 113.
4. *Idem, J. Mater. Sci.* **25** (1990) 5043.
5. B. BUDIANSKY and R. J. O'CONNELL, *Int. J. Solids Struct.* **12** (1976) 81.
6. A. HOENIG, *ibid.* **15** (1979) 137.
7. N. LAWS and J. R. BROCKENBROUGH, *ibid.* **23** (1987) 1247.
8. D. P. H. HASSELMAN and J. P. SINGH, *Amer. Ceram. Soc. Bull.* **58** (1979) 856.
9. T. YOKOBORI and M. ICHIKAWA, *J. Phys. Soc. Jpn.* **19** (1964) 2341.
10. W. R. DELAMETER, G. HERRMANN and D. M. BARNETT, "Solid by a Rectangular Array of Cracks", *J. Appl. Mech., Trans. ASME* **43** (1975) 74.
11. J. J. MECHOLSKY Jr, S. W. FREIMAN and R. W. RICE, *J. Amer. Ceram. Soc.* **60** (1977) 114.
12. H. P. KIRCHNER and E. D. ISSACSON, *ibid.* **65** (1982) 55.
13. H. P. KIRCHNER, *ibid.* **67** (1984) 127.
14. *Idem, ibid.* **67** (1984) 347.
15. T. J. LARCHUK, J. C. CONWAY Jr and H. P. KIRCHNER, *ibid.* **68** (1985) 209.
16. J. D. B. VELDKAMP, N. HATTU and G. de WITH, "High Temperature Scratching of Some Brittle Materials", in "Fracture Mechanics of Ceramics", Vol. 5, edited by R. C. Bradt, A. G. Evans, D. P. H. Hasselman and F. F. Lange (Plenum, New York, 1983) pp. 121–144.
17. D. B. MARSHALL, in "Fracture in Ceramic Materials; Toughening Mechanisms, Machining Damage, Shock", edited by A. G. Evans (Noyes, Park Ridge, New Jersey, 1984) pp. 190–220.
18. B. R. LAWN, A. G. EVANS and D. B. MARSHALL, *J. Amer. Ceram. Soc.* **63** (1980) 574.
19. B. R. LAWN and M. V. SWAIN, *J. Mater. Sci.* **10** (1975) 113.
20. B. R. LAWN and D. B. MARSHALL, *J. Amer. Ceram. Soc.* **62** (1979) 347.
21. G. R. ANSTIS, P. CHANTIKUL, B. R. LAWN and D. B. MARSHALL, *ibid.* **64** (1981) 533.
22. B. R. LAWN and E. R. FULLER, *J. Mater. Sci.* **10** (1975) 2016.
23. D. B. MARSHALL and B. R. LAWN, *ibid.* **14** (1979) 2001.
24. J. F. KALTHOFF and D. A. SHOCKNEY, *J. Appl. Phys.* **48** (1977) 986.
25. A. G. EVANS, *ibid.* **49** (1978) 3304.
26. E. D. CASE, in "Fracture Mechanics of Ceramics", Vol. 7, edited by R. C. Bradt, A. G. Evans, D. P. H. Hasselman and F. F. Lange (Plenum, New York, 1983) pp. 211–222.
27. E. CASE and A. G. EVANS, in "Fracture in Ceramic Materials; Toughening Mechanisms, Machining Damage, Shock", edited by A. G. Evans (Noyes, Park Ridge, New Jersey, 1984) pp. 404–415.
28. Y. KIM and E. D. CASE, *J. Mater. Sci.* **28** (1993) 1901.
29. *Idem, ibid.* **28** (1993) 1910.
30. B. D. AGARWAL and L. J. BROUTMAN, "Analysis and Performance of Fiber Composites" (Wiley, New York, 1980) pp. 20–26.

31. M. V. SWAIN, *J. Amer. Ceram. Soc.* **73** (1990) 621.
32. C. C. CHIU and E. D. CASE, *Mater. Sci. Engng* **A132** (1991) 39.
33. E. VOLTERRA and E. C. ZACHMANOGLOU, "Dynamics of Vibrations" (Merrill, Columbus, Ohio, 1965) pp. 321–322.
34. S. K. CLARK, "Dynamics of Continuous Elements" (Prentice Hall, Englewood Cliffs, New Jersey, 1972) pp. 75–87.
35. S. P. TIMOSHENKO and D. H. YOUNG, "Strength of Materials", 4th Edn (Van Nostrand Reinhold, Princeton, 1962) pp. 113–115.

Received 27 April
and accepted 17 June 1992